Digestibility of resistant starch type 3 is affected by crystal type, molecular weight and molecular weight distribution

Klostermann, C E; Buwalda, P L; Leemhuis, H; de Vos, P; Schols, H A; Bitter, J H

Published in:
Carbohydrate Polymers

DOI:
10.1016/j.carbpol.2021.118069

Publication date:
2021

Carbohydrate Polymers 265 (2021) 118069

Contents lists available at ScienceDirect

Carbohydrate Polymers

journal homepage: www.elsevier.com/locate/carbpol

Digestibility of resistant starch type 3 is affected by crystal type, molecular weight and molecular weight distribution

C.E. Klostermann [a], P.L. Buwalda [a,b], H. Leemhuis [b], P. de Vos [c], H.A. Schols [d], J.H. Bitter [a,*]

[a] Biobased Chemistry and Technology, Wageningen University & Research, Bornse Weilanden 9, 6708 WG Wageningen, the Netherlands
[b] Coöperative AVEBE u.a., P.O. Box 15, 9640 AA Veendam, the Netherlands
[c] Immunoendocrinology, Division of Medical Biology, Department of Pathology and Medical Biology, University of Groningen and University Medical Centre Groningen, Groningen, Hanzeplein 1, 9700 RB Groningen, the Netherlands
[d] Laboratory of Food Chemistry, Wageningen University & Research, Bornse Weilanden 9, 6708 WG Wageningen, the Netherlands

ARTICLE INFO

Keywords:
Resistant starch type 3
Dietary fiber
α-glucan
Prebiotics
HPSEC

ABSTRACT

Resistant starch type 3 (RS-3) holds great potential as a prebiotic by supporting gut microbiota following intestinal digestion. However the factors influencing the digestibility of RS-3 are largely unknown. This research aims to reveal how crystal type and molecular weight (distribution) of RS-3 influence its resistance. Narrow and polydisperse α-glucans of degree of polymerization (DP) 14–76, either obtained by enzymatic synthesis or debranching amylopectins from different sources, were crystallized in 12 different A- or B-type crystals and *in vitro* digested. Crystal type had the largest influence on resistance to digestion (A >>> B), followed by molecular weight (Mw) (high DP >> low DP) and Mw distribution (narrow disperse > polydisperse). B-type crystals escaping digestion changed in Mw and Mw distribution compared to that in the original B-type crystals, whereas A-type crystals were unchanged. This indicates that pancreatic α-amylase binds and acts differently to A- or B-type RS-3 crystals.

1. Introduction

Resistant starch (RS) is starch that resists digestion in the small intestine by human digestive enzymes and therefore ends up in the colon. In the colon RS will be fermented and may even act as a prebiotic by positively influencing beneficial gut microbiota (Fuentes-Zaragoza et al., 2011; Haenen et al., 2013; Zaman & Sarbini, 2016). Recently, it was shown that RS also may directly interact with the immune system to activate several immune responses (Bermudez-Brito, Rosch, Schols, Faas, & de Vos, 2015; Lépine et al., 2018). Five different types of RS exist: physically inaccessible starch (RS-1), native starch granules (RS-2), retrograded starch (RS-3), chemically modified starch (RS-4) and amylose-lipid complexes (RS-5) (Birt et al., 2013; Fuentes-Zaragoza et al., 2011). RS-3 is of interest as food ingredient since it is thermally stable (Haralampu, 2000) and can easily be added to foods as dietary fiber. RS-3 preparations can be made by debranching amylopectins to short chain α-glucans followed by controlled crystallization (Cai & Shi, 2014). However, to be able to act as dietary fibre, RS-3 preparations should be resistant to enzymatic digestion in the small intestine. Recently, it was suggested that RS-3 may be resistant to digestion due to slow enzyme binding of pancreatic α-amylase to the RS-3 crystals in combination with slow catalytic hydrolysis (Dhital, Warren, Butterworth, Ellis, & Gidley, 2017). However, it is not yet clear which physicochemical characteristics of RS-3 cause the resistance to digestion. Differences in digestibility of RS-3 preparations might be caused by characteristics like crystal type and molecular weight (distribution) of the crystallized α-glucans.

Resistant starch type 3 (RS-3) preparations or so-called short chain α-glucan crystals can be produced by gelatinizing starch at elevated temperatures followed by slow cooling, which results in recrystallization of the starch. The crystals formed by recrystallization can be recognized as A-type or B-type, as measured by X-ray diffraction (Gidley & Bulpin, 1987; Kiatponglarp, Tongta, Rolland-Sabate, & Buleon, 2015; Nishiyama, Putaux, Montesanti, Hazemann, & Rochas, 2010). Whether A- or B-type crystals are formed depends on the chain length of the α-glucan, concentration during crystallization and temperature of crystallization (Buleon, Veronese, & Putaux, 2007; Creek, Ziegler, & Runt, 2006; Kiatponglarp et al., 2015; Pfannemuller, 1987). In addition, RS-3 preparations differing in crystal type can be formed using different solvents like acetone, ethanol or polyethylene glycol (Huang et al.,

* Corresponding author.
E-mail address: harry.bitter@wur.nl (J.H. Bitter).

https://doi.org/10.1016/j.carbpol.2021.118069
Received 17 November 2020; Received in revised form 6 April 2021; Accepted 7 April 2021
Available online 16 April 2021

2019; Kobayashi, Kimura, Naito, Togawa, & Wada, 2015; Montesanti et al., 2010). *in vitro*, native A-type starches are easier to digest compared to native B-type starches (Martens, Gerrits, Bruininx, & Schols, 2018). In contrast, research on digestibility of retrograded short chain α-glucans has shown that retrograded A-type crystals are more resistant to digestion than retrograded B-type crystals (Cai & Shi, 2013, 2014).

In addition to crystal type, average molecular weight also affects resistance to digestion of RS-3 preparations. Most research on RS-3 is performed by crystallization of debranched amylopectins resulting in a wide range of short chain linear α-1,4 linked glucans (Cai & Shi, 2014; Kiatponglarp et al., 2015). By choosing waxy starches of different botanical sources, variations in average chain length (DPn) can be achieved after debranching (Cai & Shi, 2010). For example, debranched waxy maize starch has a DPn of 24, waxy wheat of DPn 22 and waxy potato of DPn 32 (Cai & Shi, 2010). In addition, starches can be modified by branching enzymes or by amylomaltases, due to which amylopectins are produced that have very short chains or elongated chains, respectively (van der Maarel & Leemhuis, 2013). After digestion of RS-3 preparations made of debranched amylopectins of different botanical sources, it was found that a higher DPn resulted in more resistance to digestion (Cai & Shi, 2010).

However, it is largely unknown how molecular weight distribution influences the resistance to digestion of RS-3 preparations. Such a broad range of α-1,4 glucans can be obtained by debranching amylopectins, as shown for waxy wheat amylopectin resulting in chain lengths of DP 6–66 with an average of DP 22 (Cai & Shi, 2010). When such a polydisperse mixture is crystallized and subjected to digestion, it is not yet clear how the presence of different chain lengths influences the crystal formation and resistance to digestion. Previously, the effect of polydispersity on digestion was studied by debranching waxy and native rice starch. Debranching waxy rice starch results in α-glucan chains with a DP varying from 6 to 90, whereas debranching native rice starch also includes the linear amylose part, which has a DP up to 1000 (Kiatponglarp et al., 2015). It was shown that crystals produced from relatively narrow disperse debranched waxy rice starch are 10 % more resistant to digestion than crystals produced from polydisperse debranched native rice starch (Kiatponglarp, Rugmai, Rolland-Sabate, Buleon, & Tongta, 2016). Another study focussed on the fractionation of debranched waxy rice starch (polydispersity index (PI) 2.2) (Hu et al., 2020). This fractionation caused narrowing of the molecular weight distribution to a PI of 1.5 at most. After crystallization and digestion, it was shown that these crystals made of relatively narrow disperse α-glucans were 10–20 % more resistant to digestion compared to the unfractionated polydisperse crystals (Hu et al., 2020). However, the polydispersity index of before mentioned debranched and fractionated starches is still relatively high, making it hard to draw conclusions on the influence of polydispersity on crystal formation and subsequent digestibility.

In contrast to polydisperse α-1,4 glucans obtained by debranching amylopectins, narrow disperse amyloses can be enzymatically synthesized by potato glucan phosphorylase from glucose-1-phosphate (G-1-P) (Chang et al., 2018; Kobayashi et al., 2015; Roger, Axelos, & Colonna, 2000; Yanase, Takaha, & Kuriki, 2006). Potato glucan phosphorylase uses glucose-1-phosphate as a substrate and transfers the glucose residue to a primer molecule, being maltotetraose or an α-1,4 linked oligomer of DP $>$ 4 (Ohdan, Fujii, Yanase, Takaha, & Kuriki, 2006). The ratio between the glucose-1-phosphate and primer molecule determines the DPn at the end of the enzymatic synthesis. By choosing the right ratio, narrow disperse equivalents of debranched amylopectins can be synthesized that have a similar average molecular weight (Mw) but a lower polydispersity index. However, glucose-1-phosphate as substrate is quite expensive. As an alternative, the combination of sucrose and sucrose phosphorylase can be used to produce glucose-1-phosphate (Luley--Goedl & Nidetzky, 2010; Qi, You, & Zhang, 2014). Using sucrose as substrate also has shown to improve the yield of synthesis, compared to using glucose-1-phosphate directly (Ohdan et al., 2006).

The present study focusses on the effect of crystal type, Mw and Mw distribution on the resistance to digestion of RS-3 preparations. Different resistant starches were produced by debranching amylopectins (polydisperse) or through synthesis with the help of potato glucan phosphorylase and sucrose phosphorylase (narrow disperse). The ratio of G-1-P and sucrose was chosen to obtain α-1,4 linked glucans with a similar average number molecular weight (Mw_n) as the debranched amylopectins, but with a lower polydispersity index. The linear α-glucans were crystallized at different concentrations and temperatures to obtain A- and B-type crystals. These RS-3 preparations were digested to study the effect of crystal type, average Mw and Mw distribution on the resistance to digestion.

2. Materials and methods

2.1. Materials

Waxy potato starch (Eliane100), amylomaltase modified potato starch (Etenia 457) and highly branched starch of potato (Mw ±100 kDa, 8 % branch points) were provided by AVEBE (Veendam, The Netherlands). Waxy rice starch (Remyline XS) was purchased from Beneo (Mannheim, Germany). Isoamylase (EC 3.2.1.68) and maltotetraose were obtained from Megazyme (Bray, Wicklow, Ireland). Sucrose, glucose, maltose, maltotriose, pancreatin, amyloglucosidase, Lennox B (LB) medium, kanamycin sulphate, isopropyl β-D-1-thiogalactopyranoside, glucose-1-phosphate potassium salt and imidazole of high purity were obtained from Sigma-Aldrich (St. Louis, MO, USA). Bugbuster (Novagen) and benzonase nuclease were purchased from Merck (Darmstadt, Germany). MilliQ (MQ) water was used unless stated otherwise (Arium mini essential UV Ultrapure water filter, Sartorius, Göttingen, Germany).

2.2. Production of potato glucan phosphorylase and sucrose phosphorylase

The potato glucan phophorylase (PGP) (EC 2.4.1.1) and the *Bifidobacterium adolescentis* sucrose phosphorylase (SP) (EC 2.4.1.7) (van den Broek et al., 2004) were produced in *Escherichia coli* BL21 DE3 carrying the pET28a expression vector. The genes encoding PGP and SP were codon optimized for expression in *E. coli*, synthesized and cloned in pET28a by GenScript (Leiden, the Netherlands). The *E. coli* cells containing the PGP plasmid were grown for 16 h at 37 °C in LB medium that contained 25 μg/mL kanamycin while shaking at 200 rpm. The culture was transferred to 500 mL LB broth that contained 25 μg/mL kanamycin and kept for 2−3 h at 37 °C, shaking at 200 rpm until OD_{600} = 0.5−0.7. The culture was cooled down on ice and 0.1 mM isopropyl β-D-1-thiogalactopyranoside was added after which the culture was incubated for 24 h at 18 °C, 200 rpm. *E. coli* cells containing the SP plasmid were grown similarly until the inducer was added. To the SP culture of OD_{600} = 0.5−0.7 0.4 mM isopropyl β-D-1-thiogalactopyranoside was added and incubation was continued for 4 h at 30 °C, 200 rpm. Cells were centrifuged for 10 min at 16,000 x g, 4 °C. The cell pellets were resuspended in Bugbuster, causing lysis of the *E. coli* cells, and supplemented with benzonase nuclease, according to the company protocol. The lysed cells were centrifuged for 10 min at 16,000 x g, 4 °C. The supernatant was decanted and stored for 30 min at 60 °C. This suspension was centrifuged and the supernatant was filtered over an 0.2 μm filter to obtain a sterile cell-free enzyme extract. The enzymes were purified using a His-Tag purification column, according to the company protocol (GE Healthcare Life Sciences, Amersham, United Kingdom). Sample and washing buffer contained 20 mM imidazole and elution of pure enzymes was performed with 800 mM imidazole. The final PGP or SP concentration was determined by the Bradford protein assay (Bradford, 1976).

2.3. Production of polydisperse α-1,4 linked glucans

Highly branched potato starch (HBPS), waxy potato starch (WPS), amylomaltase modified potato starch (AMPS) and waxy rice starch (WRS) were suspended in a 20 mM sodium acetate buffer of pH 5 and autoclaved. The solutions were cooled to 40 °C and isoamylase was added (8 U/g). The amylopectins were debranched for 48 h at 40 °C, 100 rpm and freeze dried to produce debranched HBPS (dHBPS), WPS (dWPS), AMPS (dAMPS) and WRS (dWRS).

2.4. Enzymatic synthesis of narrow disperse α-1,4 linked glucans

For studying reaction dynamics of PGP and SP sucrose and dHBPS were mixed at 105 mM in a molar ratio of 20/1 in a 30 mM sodium phosphate buffer of pH 7.0. His-tag purified PGP and SP were added (25 μg/mL) and the mixtures were incubated at 50 °C, 100 rpm in a shaking incubator. After 0, 0.5, 1 and 4 h a 50 μL sample was taken for chemical analysis (section 2.7) and heated for 15 min at 100 °C to inactivate the enzymes. For further incubations sucrose and dHBPS were mixed at 105 mM in a molar ratio of 2/1, 5/1, 20/1 and 65/1 in a 30 mM sodium phosphate buffer of pH 7.0. His-tag purified PGP and SP were added (6.25 μg/mL) and samples were incubated for 24 h at 50 °C, 100 rpm in a shaking incubator. After 24 h of incubation, the remaining samples were freeze-dried and washed with cold MQ and 80 % ethanol to remove salts, enzymes and small sugars and freeze-dried again to yield purified sG2 (2/1), sG5 (5/1), sG20 (20/1) and sG65 (65/1).

2.5. Crystallization of poly- and narrow disperse α-1,4 linked glucans

Poly- and narrow disperse α-glucans of similar DPn were suspended in MQ in different concentrations: dHBPS: 40 %w/w; sG2, dWRS and sG5: 30 %w/w; dWPS and sG20: 10 %w/w; dAMPS and sG65: 5 % w/w. The suspensions were autoclaved and stored at 80 °C prior to crystallization. Half of the dHBPS, sG2, dWRS and sG5 samples were stored for 24 h at 50 °C to produce A-type crystals, according to Cai and Shi (2014). The other half of dHBPS, sG2, dWRS and sG5 were immediately cooled on ice and stored for 24 h at 4 °C to produce B-type crystals, similar to the method proposed by Cai and Shi (2014). In addition, dWPS, sG20, dAMPS and sG65 were also immediately cooled on ice and stored for 24 h at 4 °C, to produce B-type crystals. After 24 h storage, the samples were centrifuged for 10 min at 7000 x g, 4 °C and washed with cold MQ and 80 % ethanol. The supernatants were decanted and pellets containing crystallized α-1,4 linked glucans were dried for 48 h at 40 °C. Crystallization yield was calculated as (total mass after crystallization) / (mass at start) * 100 %.

2.6. Digestion of RS-3 preparations

Digestion was performed according to Martens et al. with minor modifications (Martens et al., 2018). RS-3 preparations were suspended in 100 mM sodium acetate buffer pH 5.9 at 20 mg/mL. Pancreatin solution was prepared according to Martens et al. (2018), without addition of invertase. Samples were incubated for 0, 20, 60, 120 and 240 min and enzymes were inactivated by heat treatment for 15 min at 100 °C. After 360 min of incubation, the samples were centrifuged for 10 min at 19,000 x g, 4 °C and the enzymes in the supernatant were inactivated by heat treatment for 15 min at 100 °C. The remaining pellet was washed twice with MQ and oven-dried at 40 °C overnight. Free glucose content in the heat-treated samples was measured with the GOPOD assay from Megazyme. To study the effect of pancreatic α-amylase on the Mw distribution of dWRS-A and dWRS-B crystals, a similar method was used as described before, with some minor modifications. Pancreatin solution was prepared according to Martens et al. (2018), without addition of invertase and amyloglucosidase. Samples were incubated for 0, 20, 60 and 360 min and immediately centrifuged for 10 min at 19,000 x g, 4 °C. The pellets were washed twice with MQ and oven-dried at 40 °C overnight. The supernatants were inactivated and analysed as described before.

2.7. Molecular weight distribution of RS-3 preparations, before and after digestion

RS-3 preparations of DP < 25 were suspended in MQ at 2.5 mg/mL and dissolved by boiling. RS-3 preparations of DP > 32 were solubilised in 1 M NaOH at 60 mg/mL sample. The samples were diluted to 2.5 mg/mL and neutralized by addition of 1 M HCl. Samples were centrifuged at 19,000 x g for 10 min and the supernatant was analysed with a Dionex Ultimate 3000 system (Sunnyvale, USA). Ten μL sample was injected on a column set that consisted of three in series connected TSKgel SuperAW columns (SuperAW4000 6.0 × 150 mm, 6 μm; SuperAW3000 6.0 × 150 mm, 4 μm; SuperAW2500 6.0 × 150 mm, 4 μm) (Tosoh Bioscience, Tokyo, Japan) with a TSKgel guard column (SuperAW-L 4.6 × 35 mm, 7 μm). Elution was performed with 0.6 mL/min and 0.2 M $NaNO_3$, at 55 °C. Detection was performed with a Shodex RI-101 detector (Showa Denko, K.K., Kawasaki, Japan). Calibration of the column was performed with pullulan standards (Supelco, Bellefonte, USA).

From the HPSEC-RI results, DPn, DPm and PI were calculated using pullulan calibration. Intensities were normalized and base-line corrected, after which Mn was calculated using formula 1. Mm was calculated using formula 2 and PI was calculated by dividing Mm over Mn. The retention time frame of each peak was taken into account to calculate Mn and Mm.

$$1)\ Mn = \sum Mw_p * I_n$$

$$2)\ Mm = \frac{\sum Mw_p^2 * I_n}{Mn}$$

In which Mn is the number based average Mw, whereas Mm is the mass based average Mw, Mw_p is the Mw based on pullulan calibration and I_n is the normalised and base-line corrected intensity at retention time x.

Samples were diluted to 0.25 mg/mL and centrifuged at 19,000 x g for 10 min. The supernatant was analysed using an ICS 3500 HPAEC system from Dionex, in combination with a CarboPac PA-1 (2 × 250 mm) column, with a CarboPac PA-1 guard column (Dionex). The detector used was an electrochemical Pulsed Amperometric detector from Dionex. Ten μL of supernatant was injected on the column and eluted by a gradient consisting of eluent A (0.1 M NaOH solution) and eluent B (1 M NaOAc in 0.1 M NaOH). The gradient used was 2.5–40 % B (0−50 min), 40–100 % B (50−65 min), 100 % B (65−70 min), 2.5 % B (70−85 min). Elution was performed with 0.3 mL/min at 25 °C. A calibration curve of 5−10 μg/mL of malto-oligosaccharides (DP 1 – DP 7) was run for quantification. Data analysis was performed with ChromeleonTM 7.2.6 software from Thermo Fisher Scientific (Waltham, Massachusetts, USA).

2.8. Crystal type determination by X-ray diffraction

Wide angle X-ray scattering (WAXS) powder diffractograms of the RS-3 preparations were measured on a Bruker Discover D2 diffractometer (Bruker corporation, Billerica, Massachusetts, USA) using Cu radiation (1.54 Å) in the reflection geometry in the angular range of 5–35 2°θ with a step size of 0.051°2θ and 1 s per step in a rotating stage of 10°/min. Detection was performed with Lynxeye XE-T (Bruker corporation). XRD diffractograms were background corrected and normalized.

2.9. Scanning Electron Microscopy of RS-3 preparations

Crystal morphology was determined with Scanning Electron Microscopy (SEM) (Magellan 400, FEI, Eindhoven, The Netherlands) at the

Wageningen Electron Microscopy Center (WEMC). The RS-3 preparations were attached to sample holders containing carbon adhesive tabs (EMS, Washington, USA) and coated with 12 nm tungsten (EM SCD 500, Leica, Vienna, Austria). The crystals were analysed with a field emission SEM at 2 kV and magnification of 10,000 times.

3. Results & discussion

3.1. Production of narrow disperse α-glucans

Narrow disperse α-glucans were enzymatically synthesized by potato glucan phosphorylase (PGP) and sucrose phosphorylase (SP) using debranched highly branched potato starch (dHBPS) as primer molecule and sucrose as a substrate. The synthesis was followed over time and analysed by HPAEC-PAD (Fig. 1).

At t = 0 min, the chromatogram shows several peaks which can be identified as malto-oligomers of dHBPS and G-1-P formed after enzymatic hydrolysis of sucrose by SP (Fig. 1). The figure inset shows peaks that can be identified as sucrose, fructose and glucose. Over time (t = 30, t = 60, t = 240 min), the sucrose was hydrolysed and fructose formed, showing activity of SP. The PAD signal of G-1-P increased and decreased over time, whereas the malto-oligomers of dHBPS were elongated up to at least DP 40 over time, indicating PGP activity. Due to this shift in malto-oligomers towards higher DP's over time, it can be stated that PGP favoured to elongate the smallest malto-oligomer present (DP > 4). Although literature states that based on the polydispersity index, enzymatically synthesized α-glucans are narrow disperse (Kobayashi et al., 2015; Ohdan et al., 2006), this result shows that still a rather broad mixture of α-glucans was formed after enzymatic synthesis.

Sucrose and dHBPS were incubated at a ratio of 2/1, 5/1, 20/1 and 65/1 with PGP and SP to synthesize α-glucans of DP 14 (sG2), 18 (sG5), 32 (sG20) and 78 (sG65). The synthesis yields after 24 h of incubation was between 65–85 %. The average Mw and polydispersity index (PI) of the synthesized and purified α-glucans were analysed and calculated after size exclusion chromatography (Table 1, Supplementary Fig. 1).

The results show that the Mw of the final α-glucan after enzymatic synthesis increased with the sucrose/dHBPS ratio (Table 1). The higher the sucrose/dHBPS molar ratio, the more G-1-P was available for the reaction and thus the higher Mw α-glucans were formed, as stated in literature previously (Ohdan et al., 2006). The DPn at the end of the synthesis can be predicted by the choice of primer and the ratio between substrate and primer (van der Vlist et al., 2008). The primer used in the present experiment was dHBPS which has a DPn of 12. The DP at the end of synthesis can be calculated by:

$$DP = [sucrose]/[dHBPS] + 12$$

Table 1
Average chain length (DPn) and polydispersity index (PI) of synthesized α-glucans before and after purification after 24 h one-pot incubation of sucrose and debranched HBPS in different molar ratios with potato glucan phosphorylase and sucrose phosphorylase.

Sample name	Sucrose/ dHBPS	$DPn_{t=24\ h}$	$PI_{t=24\ h}$	$DPn_{purified}$	$PI_{purified}$
sG2	2/1	13.9 ± 0.1	1.40 ± 0.01	16.3 ± 0.2	1.32 ± 0.01
sG5	5/1	15.9 ± 0.1	1.33 ± 0.01	18.2 ± 0.3	1.25 ± 0.01
sG20	20/1	29.1 ± 0.3	1.20 ± 0.00	30.7 ± 0.3	1.12 ± 0.01
sG65	65/1	74.7 ± 0.3	1.06 ± 0.01	72.0 ± 0.3	1.08 ± 0.02

As the table shows, this equation matched quite well with the results obtained. It should be noted that dHBPS has a PI of 1.51 and thus is not a monodisperse α-glucan by itself (Fig. 1, t = 0).

After synthesis, the α-glucans were purified to remove left-over sucrose, G-1-P, salts, SP and PGP. The HPSEC profiles clearly show that some small malto-oligomers were washed away during purification of sG2 and sG5 (Supplementary Fig. 2).Therefore, this purification step resulted in a lower PI, with a slightly higher DPn in case of low Mw α-glucans (sG2, sG5) and a similar DPn in case of higher Mw α-glucans (sG20, sG65).

In addition, the results show that the higher the Mw of the formed α-glucan, the lower the PI found (Table 1; eg DPn 13.9, PI 1.40 vs DPn 74.7, PI 1.06). The PI of the synthesized α-glucans is quite high, especially compared to literature that showed PI < 1.07 (Ohdan et al., 2006) or PI < 1.17 (Roger et al., 2000). However, both studies focused on synthesis of high Mw amyloses of DP >> 75, due to which lower PI values were obtained. In addition, both studies used the monodisperse primers maltotetraose (Ohdan et al., 2006) and maltohexaose (Roger et al., 2000) whereas the present study used a polydisperse debranched amylopectin as primer molecule. A previous study using glycogen phosphorylase for enzymatic synthesis was able to synthesize α-glucans of DPn 21 with a polydispersity index of 1.1, using maltopentaose as a primer molecule (Kobayashi et al., 2015).

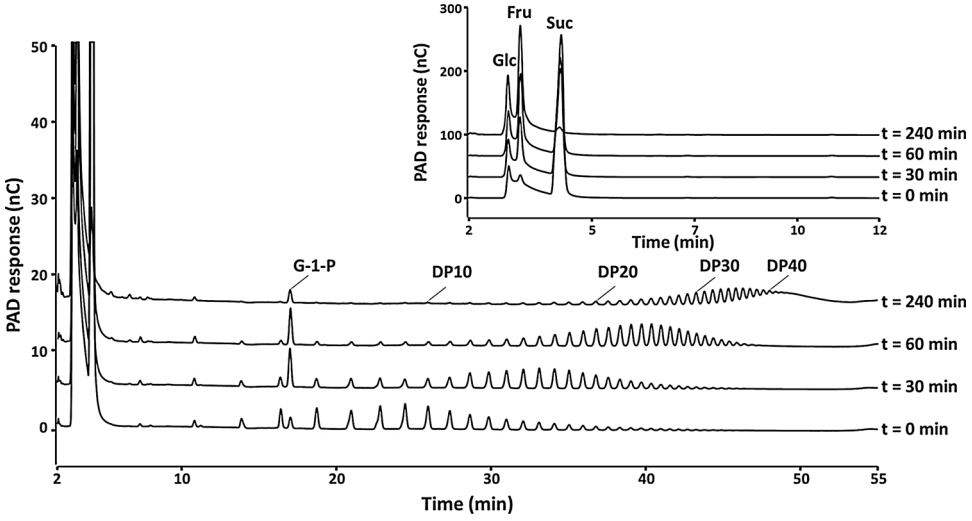

Fig. 1. HPAEC elution pattern of the one-pot incubation of sucrose and debranched HBPS (ratio 20/1) with potato glucan phosphorylase and sucrose phosphorylase during 240 min of incubation. Abbreviations used: Glc = glucose, Fru = fructose, Suc = sucrose, G-1-P = glucose-1-phosphate, DP = degree of polymerization. The inset shows the first 12 min of the chromatogram; a decrease of sucrose and an increase of fructose over time can be observed.

Although our purified narrow disperse α-glucans of DPn 16 and 18 were still not fully monodisperse, it was decided that they were different enough from their polydisperse equivalents and thus useful to study the effect of Mw distribution on resistance to digestion in RS-3.

3.2. Crystallization of narrow- and polydisperse α-glucans

In order to produce RS-3 preparations differing in Mw, PI and crystal type, the purified narrow disperse α-glucans were autoclaved and crystallized at 4 °C or 50 °C, according to Cai and Shi (2014), aiming at B-type and A-type crystals, respectively. Different types of debranched amylopectin were used as polydisperse equivalents of narrow disperse synthesized sG2, sG5, sG20 and sG65, namely: debranched highly branched potato starch (dHBPS), debranched waxy rice starch (dWRS), debranched potato starch (dWPS) and debranched amylomaltase modified potato starch (dAMPS), respectively. Crystallization was done similarly to the narrow disperse α-glucans. The α-glucans of DP ≥ 32 were only stored at 4 °C, since previous research showed that these always crystallize in a B-type polymorph, irrespectively of crystallization temperature (Cai & Shi, 2014). The crystal type of the α-glucans was determined and their Mw distribution was analysed after solubilization in NaOH (Table 2). The crystallization yield was calculated based on the recovery of crystallized molecules (Table 2).

The results from X-ray diffraction show that crystallization at 4 and 50 °C indeed resulted in the desired crystal polymorphs (Table 2). Although differences in relative intensity of the peaks were observed between the diffractograms of the crystallized α-glucans, still clear A- and B-type polymorphism could be recognized (Fig. 2). Previously, in-depth studies were performed on identification of A- and B-type peak positions of crystallized amylose (Kobayashi et al., 2015; Nishiyama et al., 2010). The XRD patterns of our crystallized α-glucans match the peak positions of Nishiyama et al. (2010), although differences in relative intensities were observed.

Debranching of amylopectins of selected sources followed by crystallization resulted in crystals having similar Mw and crystal type compared to their synthesized equivalents, but differing in polydispersity index. Despite large differences in PI and Mw distribution (Supplementary Fig. 3), sG20-B and dWPS-B had a comparable Mw and crystal type. The polydisperse equivalent of sG65-B (dAMPS) was found to have a much lower average Mw compared to sG65-B (Table 2). Therefore, these samples cannot be used to study the effect of PI on resistance to digestion.

Crystallization yield was found to be highly dependent on DP and crystallization temperature; at 50 °C much lower yields were obtained compared to crystallization at 4 °C for α-glucans of the same Mw (Table 2, A vs B-type crystals). In addition, the lower the DP, the lower crystallization yields were found, although lower Mw α-glucans were crystallized at higher concentrations (Table 2).

Table 2
Crystal type, Mw and Mw distribution and crystallization yield of purified narrow and polydisperse RS-3 preparations.

α-glucan	Crystal type	$DPn_{crystal}$	$PI_{crystal}$	Crystallization yield (%)
sG2-A	A	15.6 ± 0.3	1.23 ± 0.01	35 ± 1
sG2-B	B	15.2 ± 0.1	1.25 ± 0.00	86 ± 0
dHBPS-A	A	14.3 ± 0.1	1.33 ± 0.01	21 ± 1
dHBPS-B	B	14.0 ± 0.1	1.35 ± 0.00	45 ± 3
sG5-A	A	18.0 ± 0.2	1.21 ± 0.01	60 ± 2
sG5-B	B	18.0 ± 0.0	1.21 ± 0.00	89 ± 2
dWRS-A	A	21.4 ± 1.9	1.59 ± 0.01	63 ± 2
dWRS-B	B	21.9 ± 0.5	1.50 ± 0.01	79 ± 1
sG20-B	B	31.6 ± 0.3	1.14 ± 0.00	87 ± 8
dWPS-B	B	39.9 ± 0.7	2.11 ± 0.02	78 ± 10
sG65-B	B	75.6 ± 0.9	1.07 ± 0.00	97 ± 3
dAMPS-B	B	53.0 ± 2.3	1.67 ± 0.03	86 ± 4

3.3. Morphology of narrow- and polydisperse RS-3 preparations

The RS-3 preparations were analysed on their morphology by scanning electron microscopy (Fig. 3). The images clearly show differences between A- and B-type RS-3 crystals. The A-type RS-3 crystals seem to consist of very tiny substructures that had been aggregated. The narrow disperse B-type RS-3 crystals are regularly formed spherical particles, except for sample sG65-B. sG65-B crystals seem to consist of smaller particles, compared to the other narrow disperse B-type crystals. The polydisperse B-type crystals show very different appearances: dHBPS-B looks like sG2-B, which can be explained by a similar Mw and a relatively similar PI (Table 2). However, dWRS-B, dWPS-B and dAMPS-B, which differ in Mw but all have a PI ≥ 1.50 do not show a regular structure and seem to be more amorphous, although a clear crystal type was confirmed by XRD (Fig. 2).

Previously, studies were performed on crystallization of debranched amylopectins (Cai & Shi, 2013, 2014). The SEM images of the debranched waxy maize starch spherulites showed similar morphology as our narrow disperse B-type crystals (Fig. 3). In addition, Kiatponglarp et al. (2016) studied crystallization of debranched native and waxy rice starches (Kiatponglarp et al., 2016). These α-glucans all crystallized in a B-type polymorph, but showed very different appearances. Their native rice starch crystals showed a rough surface morphology, similar to our sG65 crystals (Kiatponglarp et al., 2016). Also, Zeng, Zhu, Chen, Gao, and Yu (2016)) studied morphology of crystallized α-glucans produced by different drying methods (Zeng et al., 2016). Their air-dried debranched waxy rice starch crystals greatly resembled our air-dried dWRS crystals. In addition, narrow disperse α-glucans were previously crystallized to A- and B-type crystals (Kobayashi et al., 2015). The B-type crystals that had similar Mw values compared to the crystals in the current study had the same morphology as we observed. However, the previously produced A-type crystals showed a much more structured morphology, which can be explained by precipitation with acetone (Kobayashi et al., 2015) instead of self-assembly as in the present study. It should be noted that our study focused on the retrogradation of α-glucans from aqueous environment, mimicking resistant starch formation during cooking in a simplified way.

To summarize, 12 different RS-3 preparations were produced that differed in crystal type (A/B), Mw (DPn ± 15, 20, 32 and 75) and PI (≤ 1.25 or ≥1.35). These RS-3 preparations were used to study the effect of crystal type, Mw and Mw distribution on resistance to digestion.

3.4. Digestibility of narrow and polydisperse RS-3 preparations

In order to investigate the effect of crystal type, Mw and Mw distribution on the resistance to digestion, the twelve narrow and polydisperse RS-3 preparations were digested according to Englyst et al. and Martens et al. (Englyst, Kingman, & Cummings, 1992; Martens et al., 2018) (Fig. 4).

3.4.1. RS-3 A-type crystals are more resistant to digestion than B-type crystals

Firstly, the results show that both dHBPS-A and dHBPS-B were digested completely within 360 min and thus these RS-3 preparations cannot be considered as RS-3, although being retrograded, insoluble and showing a clear crystal type (Figs. 4A, 2). However, the results do show that dHBPS-A (DPn 14) was slower digested than dHBPS-B (DPn 14), indicating that B-type crystals were easier digested than A-type crystals. Moreover, the narrow disperse A-type crystals (sG2-A, DPn 15) were digested for 20 % during the first 60 min of digestion, whereas the narrow disperse B-type crystals (sG2-B, DPn 15) were digested for 80 % (Fig. 4A). Slower digestion of A-type crystals compared to B-type crystals was also observed for poly- and narrow disperse A- and B-type RS-3 preparations of DPn 18–22 (Fig. 4B). Therefore, it can be stated that A-type crystals were more resistant to digestion than B-type crystals, comparing A- and B-type digestibility within one chain length. This

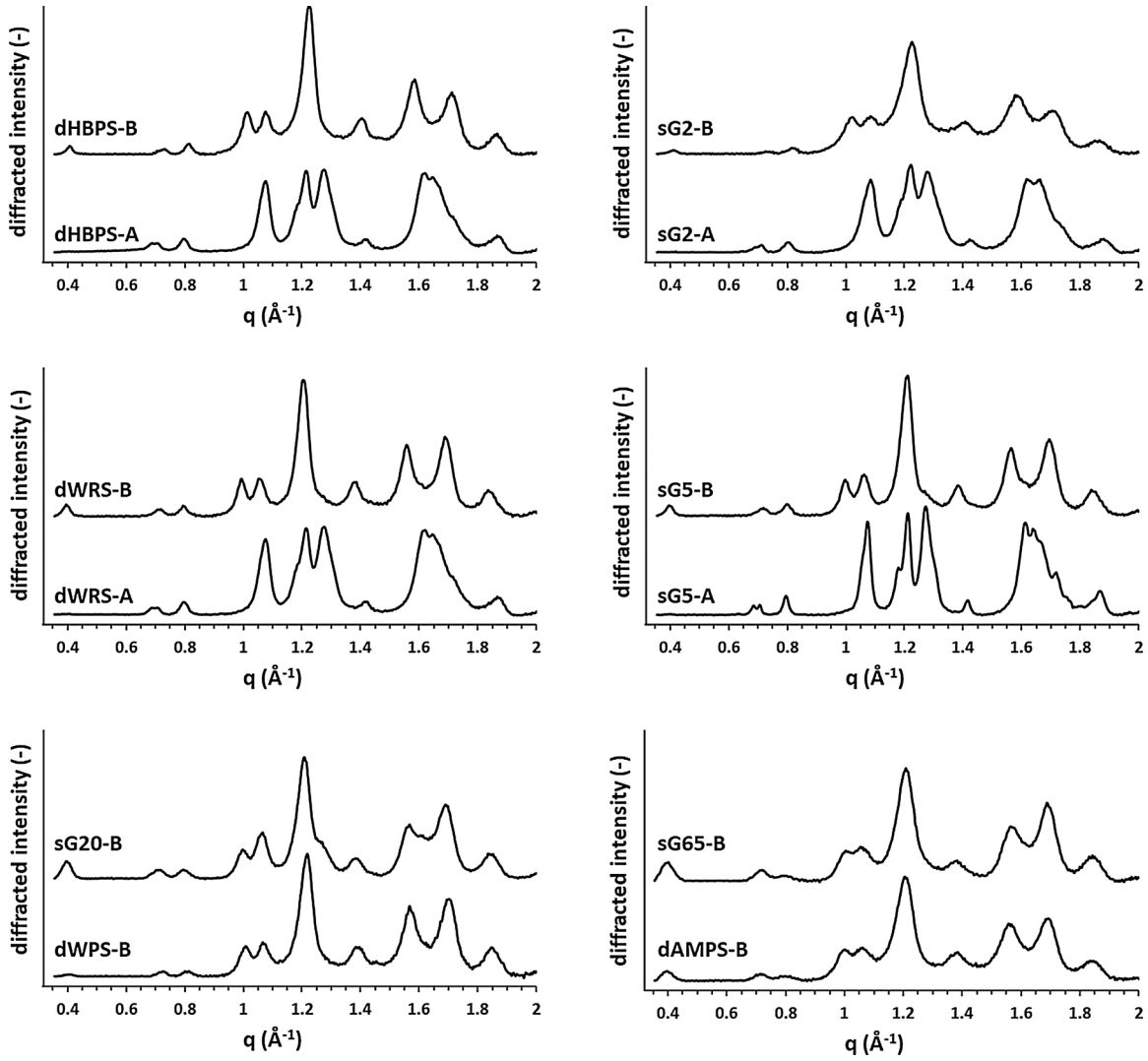

Fig. 2. XRD profiles of narrow and polydisperse RS-3 preparations.

aligns with previous research showing that retrograded A-type crystals of similar chain length were more resistant to digestion than B-type crystals (Cai & Shi, 2014).

3.4.2. RS-3 preparations of longer chain length α-glucans are more resistant to digestion than that of shorter chain length, irrespectively of crystal type

The results also show that A-type crystals made of longer chain length α-glucans were more resistant to digestion than A-type crystals made of shorter chain length α-glucans (dHBPS-A vs dWRS-A, sG2-A vs sG5-A, Fig. 4A & B, Table 3). In addition, polydisperse B-type crystals made of longer chain length α-glucans were also more resistant to digestion than polydisperse B-type crystals made of shorter chain length α-glucans (dHBPS-B, dWRS-B, dWPS-B, dAMPS-B (Fig. 4A & B & C & D), Table 3). Moreover, narrow disperse B-type crystals of longer DP were also more resistant to digestion, although a minor difference in final digestibility was observed between sG20-B and sG65-B (sG2-B, sG5-B, sG20-B, sG65-B) (Fig. 4, Table 3). Therefore, it can be stated that RS-3 preparations made of longer chain length α-glucans were more resistant to digestion, compared to RS-3 preparations made of shorter chain length α-glucans, irrespectively of crystal type.

3.4.3. RS-3 preparations of narrow disperse α-glucans are slightly more resistant to digestion than that of polydisperse α-glucans

Lastly, the results show that RS-3 preparations made of narrow disperse α-glucans were more resistant to digestion than RS-3 preparations made of polydisperse α-glucans, although no major differences were found for most samples (Fig. 4A (dHBPS-B vs sG2-B), B, Table 3). A-type crystals with a low PI and low Mw were found to be more resistant than their polydisperse equivalent (dHBPS-A vs sG2-A or dWRS-A vs sG5-A, Table 3). Interestingly, sG2-A was much more resistant to digestion than its polydisperse counterpart dHBPS-A (23 vs 100 % digestible, respectively). This, although their Mw and PI only differed slightly from each other (Table 2). We hypothesize that a lower limit of DPn 15 is needed to remain connected to the A-type crystal during enzymatic digestion. Because of this, the dHBPS-A crystal was 100 % digestible, whereas the sG2-A crystal was only digestible for 23 % after 360 min. B-type crystals with a low PI and DPn 32 (sG20-B) were much more resistant to digestion than their polydisperse equivalents (dWPS-B), with a difference in PI of 0.97 (Fig. 4C, Table 2). The morphology of these crystals was very different, which might explain this difference (Fig. 3). It can be stated that narrow disperse crystals were slightly more resistant to digestion than polydisperse crystals.

3.5. Digestion affects Mw (distribution) of especially B-type RS-3 crystals that remain after digestion

The RS-3 crystals that resist digestion in the small intestine will arrive in the colon where they might be degraded and fermented by

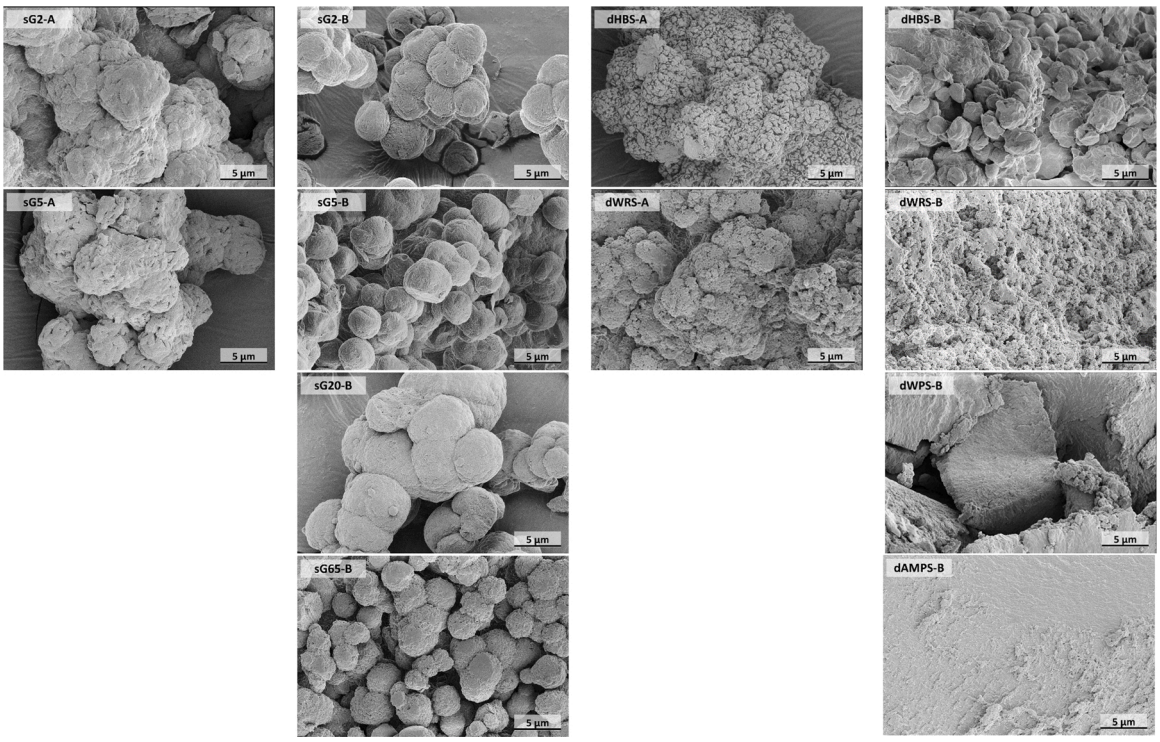

Fig. 3. Scanning electron microscopic images of RS-3 preparations differing in Mw, Mw distribution and crystal type. Sample codes are explained in Table 2.

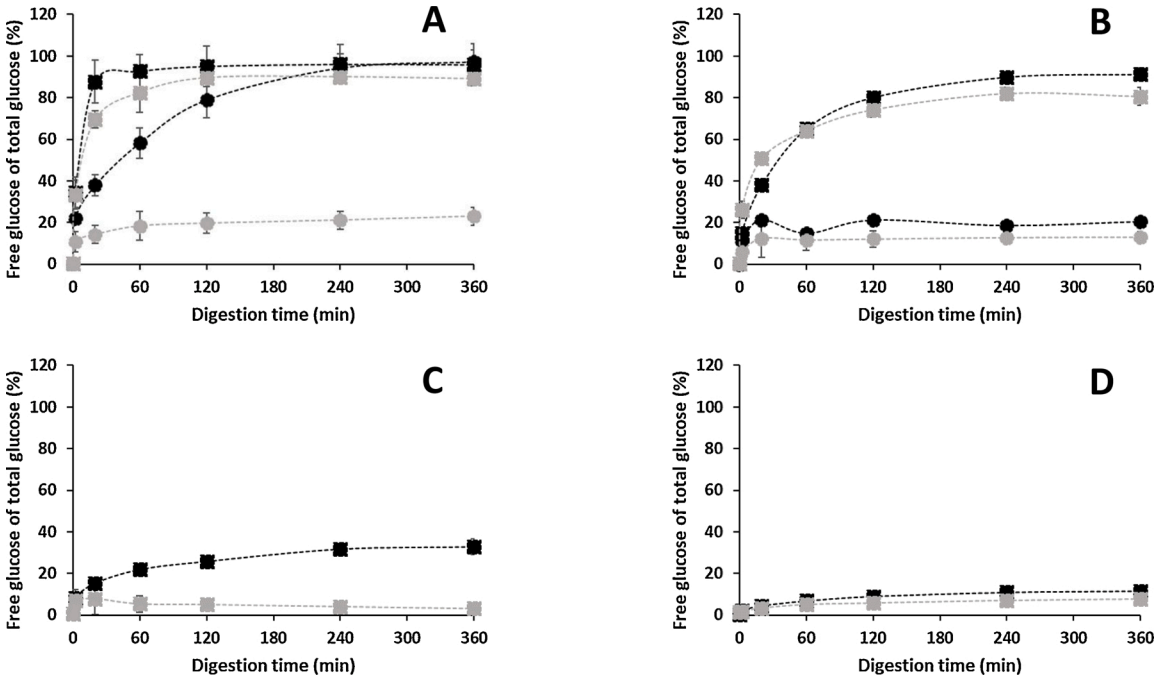

Fig. 4. In vitro digestion profiles of narrow and polydisperse RS-3 preparations. A (DP ± 15): dHBPS, sG2; B (DP ± 20): dWRS, sG5; C (DP ± 32): dWPS, sG20; D (DP ≥ 50): dAMPS, sG65. □ = B-type crystal, ○ = A-type crystal. Digestibility curves of dHBPS are from 5 individually produced samples, all others are from in triplicate produced samples, all digested in duplicate.

specific gut microbiota. To examine whether these remaining RS-3 crystals had physically been changed due to the attack of pancreatic α-amylase, the Mw and PI of the remaining crystals that escaped digestion was analysed (Table 3).

The results show that for most remaining RS-3, digestion only had a minor effect on the Mw and PI compared to the undigested crystalline α-glucans (sG2-A, sG5-A, dWRS-A, sG20-B, dWPS-B) (Tables 2 & 3). This indicates that in most digestions, pancreatic α-amylase hydrolysed some crystals completely, whereas others were completely untouched. However, for some other samples a change in Mw and PI can be observed (sG5-B, dWRS-B, sG65-B). sG5-B crystals decreased in Mw, whereas their PI remained similar after digestion. This indicates that for sG5-B, all crystals were hydrolysed to a certain extent, without a preference for either longer or shorter α-glucans within the crystal. Furthermore,

Table 3
Molecular weight and polydispersity (changes) of RS-3 crystals remaining after 360 min of *in vitro* digestion, together with total digestibility (%).

Sample name	Digestibility (%)	$DPn_{crystal}$	$PI_{crystal}$	$\Delta DPn_{crystal}$ (%)	$\Delta PI_{crystal}$ (%)
sG2-A	23 ± 4	15.2 ± 0.5	1.25 ± 0.01	−2.7	1.5
sG2-B	89 ± 2	n.a.	n.a.	n.a.	n.a.
dHBPS-A	100 %	n.a.	n.a.	n.a.	n.a.
dHBPS-B	100 %	n.a.	n.a.	n.a.	n.a.
sG5-A	13 ± 3	17.0 ± 0.8	1.22 ± 0.01	−5.9	1.5
sG5-B	81 ± 4	12.7 ± 2.6	1.22 ± 0.03	−41.9	1.1
dWRS-A	20 ± 0	24.8 ± 0.3	1.53 ± 0.01	13.7	−4.1
dWRS-B	91 ± 3	18.5 ± 1.2	1.43 ± 0.06	−18.5	−4.5
sG20-B	3 ± 1	30.9 ± 0.5	1.09 ± 0.00	−2.5	−3.7
dWPS-B	33 ± 4	41.8 ± 1.5	2.01 ± 0.02	4.4	−4.7
sG65-B	8 ± 1	68.5 ± 1.2	1.10 ± 0.01	−10.1	2.6
dAMPS-B	12 ± 2	50.0 ± 0.8	1.69 ± 0.02	−6.2	1.4

dWRS-B crystals decreased in both Mw and in PI, which indicates that all crystals were hydrolysed to a certain extent and interestingly, pancreatic α-amylase caused narrowing of the PI. In contrast, sG65-B crystals also decreased in average Mw but increased slightly in PI. This indicates that pancreatic α-amylase hydrolysed some α-glucans within the sG65-B crystals to a certain extent. Probably, the hydrolysed α-glucan remained connected to the insoluble sG65-B crystal, thereby limiting further hydrolysis and therefore increasing the PI.

To understand how the digestion of dWRS A- and B-type crystals occurred, the digestion was monitored in time and remaining crystals that escaped digestion were analysed on Mw distribution (Fig. 5).

The results show that A-type crystals did not change in Mw over time. Therefore, we state that the crystals were digested in a crystal-by-crystal manner: some crystals were hydrolysed completely, whereas others were untouched. However, dWRS-B type crystals changed in Mw due to digestion: the crystals consisted of a bimodal distribution at $t = 0$, which changed slowly over time to a normal distribution after 6 h of digestion (Fig. 5).

Although activity of pancreatic α-amylase was studied extensively from a biochemistry point of view in the past, not much research is performed on the activity of pancreatic α-amylase on insoluble substrates and even less literature can be found on activity of pancreatic α-amylase on RS-3. Previously, it was revealed that human pancreatic α-amylase has two starch surface binding sites: one that binds to soluble starch molecules and another that binds to insoluble starch granules (Zhang et al., 2016). Whether this starch surface binding site is also able to bind insoluble RS-3, is still unknown.

Our research and that of others has shown that retrograded A-type crystals were more resistant to digestion than retrograded B-type crystals (Cai & Shi, 2014). As proposed by Dhital et al. (2017), digestion of retrograded starches is probably limited due to a combination of slow enzyme binding to the surface of the substrate and slow catalysis in the active site (Dhital et al., 2017). Retrograded A-type crystals have a much denser structure, containing less water molecules than B-type crystals (Buleon et al., 2007). Due to this dense structure, it might be that A-type crystals are not recognized by the surface binding sites of the enzyme. In addition, due to this dense structure, it seems likely that A-type crystals get much harder into solution compared to B-type crystals, therefore limiting enzymatic hydrolysis. Our results also show that digestion of A-type crystals reached a certain plateau value after 120 min (Fig. 4). Since we have observed that this plateau value is reached after 120 min of digestion and no change in Mw was found due to digestion, we propose that although the crystals were bound to the surface binding site, the retrograded A-type crystals are resistant to digestion due to limited catalytic activity by the enzyme; the catalytic centre of pancreatic α-amylase was unable to hydrolyse further, probably due to the dense structure of A-type crystals.

In case of B-type crystals that have a high PI, we propose that the limited digestion is related to the slow binding to the surface binding site of the enzyme rather than the catalytic activity of the enzyme, since we did not reach plateau values at 120 or even after 360 min of digestion (Fig. 4). Narrow disperse B-type crystals were shown to be more resistant to digestion compared to polydisperse B-type crystals (Fig. 4, Table 3). Because of the low PI it seems likely that crystallization of narrow disperse α-glucans resulted in more perfect crystals, compared to polydisperse α-glucans (Fig. 3). Consequently, narrow disperse α-glucans within the crystal are less likely to go into solution and are less hydrolysed, compared to crystals made of polydisperse α-glucans. Narrow disperse B-type crystals of $DP \geq 32$ were shown to be very resistant to digestion (Fig. 4). Whereas sG65-B (DP 75) did not reach a plateau value after 360 min of digestion, sG20-B (DP 32) did. Therefore, based on our results we cannot conclude whether resistance to digestion of narrow disperse B-type crystals is more related to limited binding to the surface binding site of the enzyme or to limited catalytic activity in the active site of the enzyme. Furthermore, our results have shown that RS-3 preparations produced from low Mw α-glucans ($DP \leq 14$) cannot be considered RS, since they were fully digested within 120 min, although insoluble. Unfortunately, we were not able to confirm our hypothesis on differences in digestibility mechanism by pancreatic α-amylase by SEM on these digested samples without major sample pre-treatment that might influence the outcome. However, previous research by others has not shown major differences in morphology of the α-glucan crystals due to enzymatic digestion (Ziegler, 2020).

Our research is the first that used enzymatic synthesis from sucrose for the production of RS-3 with defined and narrow distributed chain length. Twelve unique RS-3 preparations were produced of which half were enzymatically synthesized and narrow disperse. The other six RS-3 preparations were produced by debranching amylopectins of different botanical sources to obtain polydisperse equivalents of similar average Mw compared to the narrow disperse α-glucans. From these twelve samples, four A-type crystals and eight B-type crystals were produced. Because of this relatively large number of unique samples, we were able

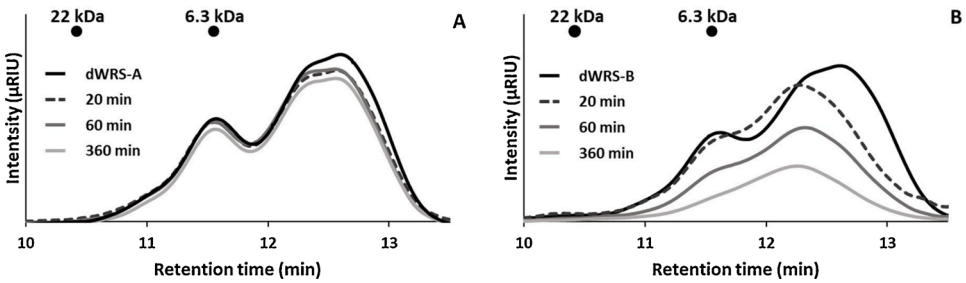

Fig. 5. HPSEC profile of A) remaining dWRS-A and B) remaining dWRS-B crystals after 0, 20, 60 and 360 min of digestion.

to study the effect of crystal type, Mw and Mw distribution on digestibility. Our rather unique approach allowed us to study for the first time the structural properties of the RS-3 crystals that escaped enzymatic hydrolysis by pancreatic α-amylase. Rather than only analysing the released glucose after *in vitro* digestion, we also analysed the remaining RS-3 crystals on Mw distribution. This makes it possible to not only predict the amount of RS-3 that enters the colon, but also to understand the substrate for beneficial gut microbes in the colon. Our results suggest that pre-digestion experiments of B-type crystals are of importance before studying the degradation and utilisation of B-type RS-3 by gut microbiota, whereas pre-digestion is hardly of any value when exploring fermentability of A-type crystals.

4. Conclusions

Our study is the first to investigate the role of crystal type, Mw and Mw distribution on the resistance to digestion of RS-3 preparations on both released glucose after *in vitro* digestion and on the crystals that escaped digestion. It has been found that A-type crystals are much more resistant to digestion than B-type crystals, potentially caused by a reduced catalytic activity of pancreatic α-amylase towards A-type crystals. A-type crystals are digested in a crystal-by-crystal manner and therefore the Mw and Mw distribution of the remaining A-type crystals does not change. Resistance to digestion of B-type crystals is potentially caused by limited binding to the surface binding site of pancreatic α-amylase. In contrast to remaining A-type crystals, remaining B-type crystals change in Mw and/or PI which might be due to surface-hydrolysis by pancreatic α-amylase. Narrow disperse RS-3 preparations are slightly more resistant to digestion than polydisperse ones and crystals made of higher DP α-glucans are more resistant than that of lower DP α-glucans, irrespectively of crystal type. In addition, RS-3 preparations of DP $\leq$ 14 cannot be considered RS, since they are 100 % digestible by pancreatic α-amylase, although insoluble. This study can help to design RS-3 preparations with a preferred degree of digestibility.

Author statement

Cynthia Klostermann: Methodology, Investigation, Writing – Original Draft; **Piet Buwalda**: Conceptualization, Supervision; **Hans Leemhuis**: Resources, Writing – Review & Editing; **Paul de Vos**: Conceptualization, Funding acquisition, Writing – Review & Editing; **Henk Schols**: Supervision, Writing – Review & Editing; **Harry Bitter**: Supervision, Writing – Review & Editing

Acknowledgements

This project is jointly funded by the Dutch Research Council (NWO), AVEBE, FrieslandCampina and NuScience as coordinated by the Carbohydrate Competence Center (CCC-CarboBiotics; www.cccresearch.nl).

Appendix A. Supplementary data

Supplementary material related to this article can be found, in the online version, at doi:https://doi.org/10.1016/j.carbpol.2021.118069.

References

Bermudez-Brito, M., Rosch, C., Schols, H. A., Faas, M. M., & de Vos, P. (2015). Resistant starches differentially stimulate Toll-like receptors and attenuate proinflammatory cytokines in dendritic cells by modulation of intestinal epithelial cells. *Molecular Nutrition & Food Research, 59*(9), 1814–1826.

Birt, D. F., Boylston, T., Hendrich, S., Jane, J. L., Hollis, J., Li, L., et al. (2013). Resistant starch: Promise for improving human health. *Advances in Nutrition, 4*(6), 587–601.

Bradford, M. M. (1976). A rapid and sensitive method for the quantitation of microgram quantities of protein utilizing the principle of protein-dye binding. *Analytical Biochemistry, 72*, 248–254.

Buleon, A., Veronese, G., & Putaux, J. L. (2007). Self-association and crystallization of amylose. *Australian Journal of Chemistry, 60*(10), 706–718.

Cai, L. M., & Shi, Y. C. (2010). Structure and digestibility of crystalline short-chain amylose from debranched waxy wheat, waxy maize, and waxy potato starches. *Carbohydrate Polymers, 79*(4), 1117–1123.

Cai, L. M., & Shi, Y. C. (2013). Self-assembly of short linear chains to A- and B-type starch spherulites and their enzymatic digestibility. *Journal of Agricultural and Food Chemistry, 61*(45), 10787–10797.

Cai, L. M., & Shi, Y. C. (2014). Preparation, structure, and digestibility of crystalline A- and B-type aggregates from debranched waxy starches. *Carbohydrate Polymers, 105*, 341–350.

Chang, R., Xiong, L., Li, M., Liu, J., Wang, Y., Chen, H., et al. (2018). Fractionation of debranched starch with different molecular weights via edible alcohol precipitation. *Food Hydrocolloids, 83*, 430–437.

Creek, J. A., Ziegler, G. R., & Runt, J. (2006). Amylose crystallization from concentrated aqueous solution. *Biomacromolecules, 7*(3), 761–770.

Dhital, S., Warren, F. J., Butterworth, P. J., Ellis, P. R., & Gidley, M. J. (2017). Mechanisms of starch digestion by alpha-amylase-Structural basis for kinetic properties. *Critical Reviews in Food Science and Nutrition, 57*(5), 875–892.

Englyst, H. N., Kingman, S. M., & Cummings, J. H. (1992). Classification and measurement of nutritionally important starch fractions. *European Journal of Clinical Nutrition, 46*(Suppl. 2), S33–50.

Fuentes-Zaragoza, E., Sanchez-Zapata, E., Sendra, E., Sayas, E., Navarro, C., Fernandez-Lopez, J., et al. (2011). Resistant starch as prebiotic: A review. *Starch-Starke, 63*(7), 406–415.

Gidley, M. J., & Bulpin, P. V. (1987). Crystallization of Maltooligosaccharides as models of the crystalline forms of starch - minimum chain-length requirement for the formation of double helices. *Carbohydrate Research, 161*(2), 291–300.

Haenen, D., Zhang, J., Souza da Silva, C., Bosch, G., van der Meer, I. M., van Arkel, J., et al. (2013). A diet high in resistant starch modulates microbiota composition, SCFA concentrations, and gene expression in pig intestine. *The Journal of Nutrition, 143*(3), 274–283.

Haralampu, S. G. (2000). Resistant starch - a review of the physical properties and biological impact of RS3. *Carbohydrate Polymers, 41*(3), 285–292.

Hu, X., Huang, Z., Zeng, Z., Deng, C., Luo, S., & Liu, C. (2020). Improving resistance of crystallized starch by narrowing molecular weight distribution. *Food Hydrocolloids, 103*, Article 105641.

Huang, Z., Zeng, Z., Gao, Y., Liu, C., Wu, J., & Hu, X. (2019). Crystallization of short-chain amylose: Effect of precipitant. *Starch-Starke, 71*(9–10), Article 1900007.

Kiatponglarp, W., Rugmai, S., Rolland-Sabate, A., Buleon, A., & Tongta, S. (2016). Spherulitic self-assembly of debranched starch from aqueous solution and its effect on enzyme digestibility. *Food Hydrocolloids, 55*, 235–243.

Kiatponglarp, W., Tongta, S., Rolland-Sabate, A., & Buleon, A. (2015). Crystallization and chain reorganization of debranched rice starches in relation to resistant starch formation. *Carbohydrate Polymers, 122*, 108–114.

Kobayashi, K., Kimura, S., Naito, P. K., Togawa, E., & Wada, M. (2015). Thermal expansion behavior of A- and B-type amylose crystals in the low-temperature region. *Carbohydrate Polymers, 131*, 399–406.

Lépine, A. F. P., de Hilster, R. H. J., Leemhuis, H., Oudhuis, L., Buwalda, P. L., & de Vos, P. (2018). Higher chain length distribution in debranched type-3 resistant starches (RS3) increases TLR signaling and supports dendritic cell cytokine production. *Molecular Nutrition & Food Research, 63*(2), Article 1801007.

Luley-Goedl, C., & Nidetzky, B. (2010). Carbohydrate synthesis by disaccharide phosphorylases: Reactions, catalytic mechanisms and application in the glycosciences. *Biotechnology Journal, 5*(12), 1324–1338.

Martens, B. M. J., Gerrits, W. J. J., Bruininx, E., & Schols, H. A. (2018). Amylopectin structure and crystallinity explains variation in digestion kinetics of starches across botanic sources in an in vitro pig model. *Journal of Animal Science and Biotechnology, 9*, 91.

Montesanti, N., Veronese, G., Buleon, A., Escalier, P. C., Kitamura, S., & Putaux, J. L. (2010). A-type crystals from dilute solutions of short amylose chains. *Biomacromolecules, 11*(11), 3049–3058.

Nishiyama, Y., Putaux, J. L., Montesanti, N., Hazemann, J. L., & Rochas, C. (2010). B–&A Allomorphic transition in native starch and amylose spherocrystals monitored by in situ synchrotron X-ray diffraction. *Biomacromolecules, 11*(1), 76–87.

Ohdan, K., Fujii, K., Yanase, M., Takaha, T., & Kuriki, T. (2006). Enzymatic synthesis of amylose. *Biocatalysis and Biotransformation, 24*(1-2), 77–81.

Pfannemuller, B. (1987). Influence of chain length of short monodisperse amyloses on the formation of A-and B-type X-ray diffraction patterns. *International Journal of Biological Macromolecules, 9*(2), 105–108.

Qi, P., You, C., & Zhang, Y.-H. P. (2014). One-pot enzymatic conversion of sucrose to synthetic amylose by using enzyme cascades. *ACS Catalysis, 4*(5), 1311–1317.

Roger, P., Axelos, M. A. V., & Colonna, P. (2000). SEC-MALLS and SANS studies applied to solution behavior of linear alpha-glucans. *Macromolecules, 33*(7), 2446–2455.

van den Broek, L. A., van Boxtel, E. L., Kievit, R. P., Verhoef, R., Beldman, G., & Voragen, A. G. (2004). Physico-chemical and transglucosylation properties of recombinant sucrose phosphorylase from Bifidobacterium adolescentis DSM20083. *Applied Microbiology and Biotechnology, 65*(2), 219–227.

van der Maarel, M., & Leemhuis, H. (2013). Starch modification with microbial alpha-glucanotransferase enzymes. *Carbohydrate Polymers, 93*(1), 116–121.

van der Vlist, J., Reixach, M. P., van der Maarel, M., Dijkhuizen, L., Schouten, A. J., & Loos, K. (2008). Synthesis of branched polyglucans by the tandem action of potato phosphorylase and Deinococcus geothermalis glycogen branching enzyme. *Macromolecular Rapid Communications, 29*(15), 1293–1297.

Yanase, M., Takaha, T., & Kuriki, T. (2006). Alpha-Glucan phosphorylase and its use in carbohydrate engineering. *Journal of the Science of Food and Agriculture, 86*(11), 1631–1635.

Zaman, S. A., & Sarbini, S. R. (2016). The potential of resistant starch as a prebiotic. *Critical Reviews in Biotechnology, 36*(3), 578–584.

Zeng, F., Zhu, S. M., Chen, F. Q., Gao, Q. Y., & Yu, S. J. (2016). Effect of different drying methods on the structure and digestibility of short chain amylose crystals. *Food Hydrocolloids, 52*, 721–731.

Zhang, X., Caner, S., Kwan, E., Li, C., Brayer, G. D., & Withers, S. G. (2016). Evaluation of the significance of starch surface binding sites on human pancreatic alpha-amylase. *Biochemistry, 55*(43), 6000–6009.

Ziegler, G. R. (2020). Enzyme-resistant starch spherulites. *Starch-Starke, 72*(7-8), Article 1900217.